



Available online at www.sciencedirect.com



Food Structure 00 (2023) 1–28

Food
Structure

Additive Manufacturing and Sensory Perception: Enhancing Sweetness in Chocolates through Structural and Compositional Modifications

Johannes Burkard^{a,b,*}, Lucas Kohler^a, Sophia Caciagli^a, Nicolas Herren^a, Mark Kozamernik^b, Saskia Mantovani^b, Erich J. Windhab^a, Christoph Denkel^b,

^a*Institute of Food, Nutrition and Health, ETH Zürich, Schmelzbergstrasse 9, 8092 Zürich, Switzerland*

^b*School of Agricultural, Forest and Food Sciences, Food Science and Management, Bern University of Applied Sciences, Länggasse 85, 3052 Zollikofen, Switzerland*

Abstract

Reducing sugar consumption is crucial for health, necessitating innovative ways to maintain taste and texture in food. Our study enhances sweetness perception in chocolate through additive manufacturing and fat modification, without increasing sugar content. Additive manufacturing was employed to adjust the spatial distribution of sugar, and cacao butter was substituted with hazelnut oil, altering the melting properties of chocolate. The study involved creating samples with a range of sugar and hazelnut oil concentrations. Our results showed that replacing cocoa butter with hazelnut oil not only affected melting speed but also amplified sweetness perception. Interestingly, adding hazelnut oil made a sample with less sugar taste as sweet as one with nearly double the sugar content. This suggests that melting characteristics can impact sweetness perception. By reordering the layers of chocolate differing in oil content, sweetness perception was increased by 11 %. However, adding complexity beyond the first layer did not enhance sweetness, suggesting less emphasis may need to be placed on structural complexity. This study offers a novel approach for sugar reduction in the food industry by modifying sensory perception through spatial sugar distribution and fat modification.

© 2023 Published by Elsevier Ltd.

Keywords: Sugar Reduction, Spatial Food Structuring, Fat Modification, Additive Manufacturing

1. Introduction

Rapidly increasing life expectancy coupled with significant lifestyle changes in western countries have led to a tremendous rise in obesity and non-communicable diseases (NCDs), such as cardiovascular diseases, diabetes, and cancer [13]. Simultaneously, there is an escalating trend towards the consumption of energy-dense and high-sugar foods coupled with reduced physical activity. The prevention of obesity and NCDs can be achieved through a variety of strategies, one of which involves reducing sugar consumption. Consequently, the demand for low-sugar foods has increased, prompting food manufacturers to explore effective sugar-reducing strategies [54, 30]. Yet, the replacement of sugar in processed foods presents a challenge, as it contributes significantly to taste and texture of many products [35, 53].

*Corresponding Author

Email address: johannes.burkard@hest.ethz.ch (Johannes Burkard)

The predominant strategy to reduce sugar in diet involves substituting sugar with sweeteners [62, 22, 30]. However, these sweeteners are often limited by their bitter or metallic aftertastes [71, 19]. Alternatively, while considering multi-sensory integration and simple sugar reduction strategies, the modification of food structure has emerged as an appealing field of study [30]. It seeks to alter perception by applying a concept known as “pulsatile stimulation”. This method exploits spatially inhomogeneous sucrose distribution with the objective of enhancing sweetness perception, thereby yielding a heightened overall sweetness perception, despite the overall sugar content remaining constant. This effect has been demonstrated in various studies involving sweet solutions [8, 9, 11, 10], multi-layered gel systems [29, 34, 50, 49], and more complex foods like bread or 3D-printed chocolate [52, 33]. For instance, a study conducted by Kistler et al. [34] involved the creation of hydrocolloid-based samples by additive manufacturing, featuring varied sweetness localization. Their findings indicated a substantial increase in sweetness perception, by up to 30 %.

To date, no study has distinctly examined the impact of anisotropically distributed sugar in complex fat-based systems on sweetness perception, while simultaneously controlling somatosensory confounders. In this research, we focused on chocolate masses with various levels of sugar (0, 23 and 42 %w/w) and hazelnut oil (0, 3 and 6 %w/w). Importantly, these masses maintained the techno-functional properties similar to the reference, except for alterations in melting properties when hazelnut oil partially replaced cocoa butter. Instrumental texture of these chocolate masses was characterized by measuring particle size distribution, melting behavior, and flow properties. Additionally, a sensory panel evaluated sensory texture, sweetness, and bitterness. Through the application of additive manufacturing, we generated anisotropically structured samples from chocolate masses varying in oil/sugar content, yet similar overall hazelnut oil and sugar loads. These samples were examined in two separate series of sensory experiments. In the first series, we combined chocolate masses with different hazelnut oil and sugar content to create layered sandwich-like samples comprised of three to five layers. Comparative profiling was conducted to evaluate maximum taste and texture perception, along with the temporal evolution of sweetness perception using time-intensity measurements. In the second series of experiments, chocolate masses with varying sugar content were utilized to create layered and cube-in-cube style samples. Progressive profiling of sweetness perception was carried out, evaluating sweetness at three stages (start, maximum, and end sweetness). Based on these results, we assessed the relevance of different mechanisms associated with pulsatile stimulation. Through this investigation, we aim to provide a deeper understanding of the potential of pulsatile stimulation to alter sensory perception in chocolate and other complex foods.

2. Materials and Methods

2.1. Chocolate Mass Manufacturing

Cacao mass (“Rondo”), cacao butter and soy lecithin (EM04B) were purchased from Max Felchlin AG (Ibach, Switzerland). Sugar was purchased from Zuckerfabriken Aarberg AG (Switzerland). Polydextrose (polydextrose type Litesse Two IP powder, Danisco AG, Netherlands) and inulin (OraftIHSI, Beneo-Orafty N.V., Belgium) were mixed at different ratios to replace sugar in chocolate masses. Hazelnut oil (Haselnussöl, Demeter, Switzerland) was used to partially replace cacao butter and to modify melting characteristics of chocolate masses.

All chocolate samples detailed in Table 1 were kept constant with regard to solids content (%w/w), and total fat content (%w/w). Sugar content in the samples spanned between 4 %w/w and 42 %w/w, achieved through replacement of sugar by a mixture of polydextrose and inulin at a consistent ratio of 2.17:1. Moreover, hazelnut oil content varied within the range of 0 to 6.25 %w/w.

All non-cocoa ingredients, i.e. polydextrose, inulin, and sucrose, were pre-mixed with melted cacao mass in a mixing device (Kenwood Major Titanium KMT056, Kenwood Swiss AG, Switzerland) for thirty minutes. Afterwards, the pre-mix was transferred to a melanger (ECGC-12SLTA, Cocoatown LLC, USA), operating at 135 rpm to refine and conche the chocolate masses. The melanger was placed in a temperature-controlled chamber at $53^{\circ}\text{C} \pm 3^{\circ}\text{C}$. After 90 minutes, melted cacao butter and/or hazelnut oil, and soy lecithin were added to the mass according to Table 1. In total, the chocolate mass was conched for seven hours.

For single mass sensory and instrumental analysis, the chocolate masses were directly quenched to 34°C in a heating chamber (Julabo TW8, Faust Laborbedarf, Switzerland). Seeded cacao butter was prepared in a SeedMaster

Table 1: Composition of chocolate masses $04_{Sc}\text{-}0_{Ho}$, $04_{Sc}\text{-}18_{Ho}$, $23_{Sc}\text{-}0_{Ho}$, $23_{Sc}\text{-}9_{Ho}$, $23_{Sc}\text{-}18_{Ho}$, $42_{Sc}\text{-}0_{Ho}$, $42_{Sc}\text{-}18_{Ho}$. The chocolate masses were labeled following the syntax *Sugar content (% w/w)_{Sc}-hazelnut oil content (%w/w)_{Ho}*, with *Sc* for sugar content in the chocolate masses, and *Ho* for the ratio of hazelnut oil to total fat in the samples.

Composition	Chocolate masses						
	$04_{Sc}\text{-}0_{Ho}$	$04_{Sc}\text{-}18_{Ho}$	$23_{Sc}\text{-}0_{Ho}$	$23_{Sc}\text{-}9_{Ho}$	$23_{Sc}\text{-}18_{Ho}$	$42_{Sc}\text{-}0_{Ho}$	$42_{Sc}\text{-}18_{Ho}$
Sugar content (% w/w)	04.15	04.15	23.00	23.00	23.00	41.71	41.71
Hazelnut content/total fat (% w/w)	00.00	17.96	00.00	08.98	17.96	00.00	17.96
Total fat (% w/w)	35.09	35.09	35.09	35.09	35.09	35.09	35.09
Cacao mass (%w/w)	50.70	50.70	50.70	50.70	50.70	50.70	50.70
Sugar (%w/w)	04.15	04.15	23.00	23.00	23.00	41.71	41.71
Inulin (%w/w)	11.83	11.83	05.55	05.55	05.55	00.00	00.00
Polydextrose (%w/w)	25.73	25.73	13.16	13.16	13.16	00.00	00.00
Cacao butter (molten) (%w/w)	06.30	00.00	06.30	03.15	00.00	06.30	00.00
Cacao butter (crystallised) (%w/w)	00.90	00.90	00.90	00.90	00.90	00.90	00.90
Hazelnut oil (%w/w)	00.00	06.30	00.00	03.15	06.30	00.00	06.30
Soy lecithin (%w/w)	00.39	00.39	00.39	00.39	00.39	00.39	00.39

60 Cryst (Bühler AG, Uzwil, Switzerland), whose workflow can be found in [45]. 1 %w/w of seeded cacao butter was
 61 added and mixed to the chocolate mass for three minutes, prior to molding into silicone shapes (Silicone Culinair®,
 62 Siliconesandmore, Netherlands) of defined geometric design (16 mm x 9.6 mm x 12.8 mm). After crystallization at
 63 15 °C, the chocolate cubes were detached from the silicone mold and stored at 4 °C. A schematic overview of the
 64 mass production can be found in Figure 1A.

65 2.2. Single Mass Characterization

66 2.2.1. Particle Size Analysis

67 Particle size distribution of the chocolate masses was measured with the Beckman laser diffraction device (13 320
 68 XR, Beckman Coulter Inc., United States). For sample preparation, the melted chocolate masses were suspended
 69 in Hydriol® SOD.24 (Hydriol AG, Wettingen, Switzerland), and the measuring device was operated with Hydriol®
 70 SOD.24. Prior to measurement, the suspended sample was sonicated at 65 Hz for two minutes in an ultrasonic bath
 71 (Elmasonic P 30 Hat, EMAG Nänikon, Schweiz) at 50 °C. The diffraction pattern was interpreted with the Fraunhofer
 72 model [16]. Three replicates per batch and sample were measured.

73 2.2.2. Rheology

74 Rheological characteristics were measured with a Rheometer (MCR 302, Anton Paar, Austria). Approximately
 75 35 g of chocolate was melted at 50 °C, thoroughly blended with 0.36 g of melted cacao butter, and transferred to a
 76 pre-heated Couette geometry (CC27, Anton Paar, Austria). The sample was pre-sheared for two minutes at a shear
 77 rate of 10 s^{-1} at 40 °C. For a logarithmic shear rate ramp ranging from 0.1 s^{-1} to 100 s^{-1} , ten data points per decade
 78 were collected. All data points were acquired under steady-state conditions. All measurements were performed in
 79 triplicates ($N = 3$), and evaluated in Origin (OriginPro 2021, 9.8.0.200).

80 2.2.3. Differential Scanning Calorimetry

81 Melting profiles of the chocolate masses were characterized by differential scanning calorimetry (DSC 3+/500,
 82 Mettler Toledo GmbH, Switzerland). An indium and a water sample were used for calibration. $5 \pm 0.2 \text{ mg}$ of tempered
 83 chocolate was weighed into a $40 \mu\text{l}$ aluminium crucible (Mettler Toledo GmbH, Switzerland). For measurement, the
 84 specimen was equilibrated at 20 °C for two minutes, followed by a heating stage to 50 °C with a heating rate of
 85 4 K/min. All samples were measured in triplicates ($N = 3$). Curve characteristics such as onset, offset, peak melting
 86 temperatures and melting enthalpy were extracted and analyzed in Origin (OriginPro 2021, 9.8.0.200).

87 2.3. Multiphase Manufacturing

88 The multiphase samples were labeled with respect to the experimental design, referring to the chocolate mass
 89 initially placed on the tongue, and the number of layers (*design_{chocolate mass on tongue | number of layers}*). The design notation
 90 consisted of the abbreviated terms for layered (abbr. *L*) or cube-in-cube (abbr. *CiC*) designs, followed by the specific

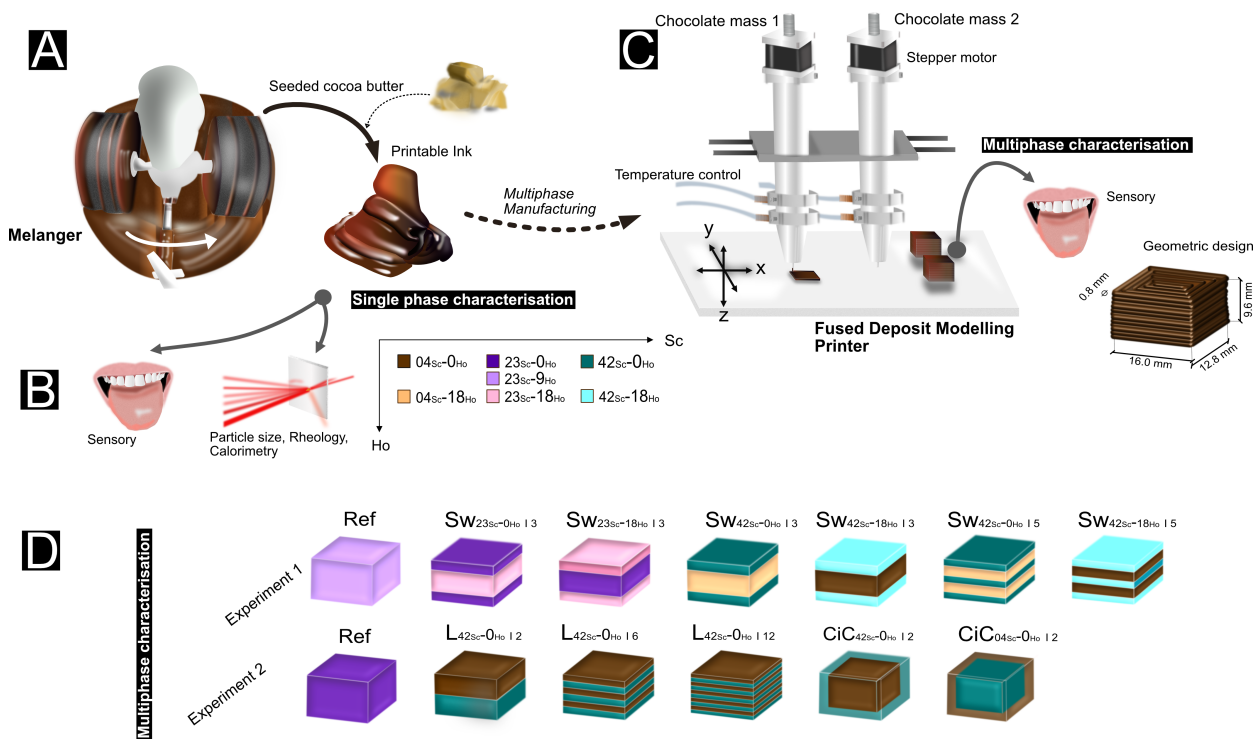


Figure 1: (A)+(C). A detailed overview of the preparation of chocolate masses and the additively manufactured multiphase samples can be found in section (D). Multiphase samples underwent two distinct sensory sessions, designated as experiment 1 and experiment 2, respectively. The fabrication of all samples was undertaken using one or two pre-characterized chocolate masses, evaluated sensorially prior to use. In addition, the chocolate masses were instrumentally evaluated by calorimetry, rheology and laser diffraction, as detailed in section (B). For experiment 1, modifications were made to the number of layers, sugar and hazelnut oil content, while ensuring a constant total sugar and hazelnut oil content. During the second session, two additional designs - referred to as *CiC* and *L* - were evaluated. This involved testing different numbers of layers in comparison to the homogeneous reference for perceived sweetness.

91 chocolate mass and the number of layers.

92
93 Initially, a sandwich design (abbr. *Sw*) was manufactured to vary the independent variables sugar concentration
94 (*Sc*), hazelnut oil content (*Ho*), and number of layers (either 3 or 5). In the sandwich designs, similar chocolate
95 masses were used at both the top and the bottom of the sample. The multiphase samples *Sw*<sub>42_{Sc}-18_{Ho}|5, *Sw*<sub>42_{Sc}-18_{Ho}|5,
96 *Sw*<sub>42_{Sc}-0_{Ho}|3, *Sw*<sub>42_{Sc}-0_{Ho}|5, *Sw*<sub>23_{Sc}-0_{Ho}|3, and *Sw*<sub>23_{Sc}-18_{Ho}|3 were prepared and compared to the *Ref* sample (23_{Sc}-9_{Ho}) (see
97 Figure 1D).</sub></sub></sub></sub></sub></sub>

98 In the follow-up session, the effect of design (*L* and *CiC*), number of layers (2, 6 and 12), and position of chocolate
99 mass within the multiphase samples on sweetness perception was investigated. Unlike the sandwich design, which
100 places identical chocolate masses at the top and bottom of the sample, the layered design presents masses of different
101 compositions at the bottom and top. This was done by combining the chocolate masses 04_{Sc}-0_{Ho} and 42_{Sc}-0_{Ho} and
102 comparing them to the homogeneous reference 23_{Sc}-0_{Ho}. The multiphase samples included *Ref* (23_{Sc}-0_{Ho}), *L*<sub>42_{Sc}-0_{Ho}|2,
103 *L*_{42_{Sc}-0_{Ho}|6, *L*_{42_{Sc}-0_{Ho}|12, *CiC*_{42_{Sc}-0_{Ho}|2, and *CiC*_{04_{Sc}-0_{Ho}|2.}}}}</sub>

104
105 The dimensions of the multiphase samples were set at 16 mm x 9.6 mm x 12.8 mm. Total sugar load (23 %w/w)
106 and hazelnut oil content (9 %w/w for experiment 1 and 0 %w/w for experiment 2) were kept consistent in relation to
107 the homogeneous reference (notated as 23_{Sc}-9_{Ho} for experiment 1 and 23_{Sc}-0_{Ho} for experiment 2, respectively). A
108 comprehensive depiction of the experimental setup and the multiphase samples is provided in Figure 1D.

109
110 The chocolate masses were transferred to stainless-steel cartridges, equipped with a 15 mm long nozzle having an
111 inner diameter of 0.8 mm (Sigrist & Partner AG, Matzingen, Switzerland). To maintain consistent product tempera-
112 ture, both cartridge and nozzle were set at 32.5 ± 0.3 °C using an aluminium jacket connected to a waterbath (Julabo
113 9153618 FP35, JULABO GmbH, Germany). Fused deposition modeling for the multiphase samples was carried out
114 using a custom-built three-axis Cartesian printer, designed by the Institute for Print Technology (Bern University of
115 Applied Sciences). Printer setup is shown in Figure 1C. It was placed within an environmental chamber (KK-1000
116 CHLT, Kambic, Slovenia) to maintain ambient temperature at 10 °C. Printer settings, including printing speed were
117 defined in the Slic3r software (Version 1.3.1). All settings are detailed in Supplementary Information 6.1. Printer
118 operation was controlled using the Repetier-Host hostware (Version 2.1.6, 2019). Following the printing process, all
119 samples were stored at 5 °C before undergoing sensory tests.

120 2.4. Sensory Analysis

121 Over 21 sessions, eight to ten participants were enlisted (ten women aged between 35 to 55 years) from the Sensory
122 Department of the Bern University of Applied Sciences (HAFL). Adapting to the constraints imposed by COVID-19
123 pandemic, experiment 2 was executed at home, while all other tests were conducted at the sensory laboratory at HAFL
124 under controlled atmosphere (20 °C ± 3°C, rH: 40 - 50%).

125 Sensory analysis consisted of two main segments. The first involved an in-depth examination of individual chocolate
126 masses, while the second part included two sensory characterizations of the 3D-printed chocolate masses, termed as
127 experiment 1 and 2. All tests were carried out by the same group of eight participants. Yet, during experiment 2, two
128 participants were substituted.

129
130 A comprehensive summary of all sensory measurements is shown in Table 2. All test sessions followed ISO
131 standards, with samples presented to participants in a randomized order, under normal light conditions, and at room
132 temperature. To ensure consistent evaluations, a standardized consumption protocol was followed. Participants were
133 instructed to place the sample in their mouth, pressing it slightly against the palate. They were allowed to swallow if
134 necessary and periodically move their tongue during consumption. Consumption was complete once the entire sample
135 was swallowed. Still water (at 25 °C) and unsalted crackers (M-Classic Microc, Migros SA, Switzerland) were pro-
136 vided to cleanse their palate between samples. Prior to being enrolled in the studies, all participants signed an general
137 informed consent document, thereby acknowledging their understanding and accepting of the study's procedures.

138 2.4.1. Single Mass characterisation

139 **Check-All-That-Apply:** At first, participants conducted a Check-All-That-Apply (CATA) test to describe the sen-
140 sory profiles of four selected chocolate masses (04_{Sc}-0_{Ho}, 04_{Sc}-18_{Ho}, 42_{Sc}-0_{Ho} and 42_{Sc}-18_{Ho}). They were presented

Table 2: Overview of all sensory tests conducted, including single mass and multiphase samples, methodology used, time order of analysis, panel and experiment details, and attributes investigated during the methodology. Training sessions always preceded evaluations. Data was analyzed following the method described in chapter 2.5.

Analysed systems	Methodology	Sequence	Training	Evaluations	Remarks	Descriptors
Single phase	Check-All-That-Apply (CATA)	1	0	1	Panel 1	Flavour (texture, taste and aroma)
	Comparative Profiling	2	3	2	Panel 1	Sweetness, smoothness, bitterness (maximum) and time of melting
Multiphase	Comparative Profiling	3	2	2	Experiment 1 Panel 1	Sweetness, smoothness, bitterness (maximum and overall) and time of melting
	Time-Intensity (TI)	4	3	2	Experiment 1 Panel 1	Sweetness (temporal)
	Progressive profiling	5	4	2	Experiment 2 Panel 2	Sweetness (start, max and end)

141 with a list of ten pre-defined attributes (see Supplementary Information 6.2), to select attributes for each sample.

142
143 **Comparative Profiling:** From CATA results, the attributes bitterness, sweetness, and smoothness, along with the
144 total melting time, were identified as most important for differentiating the chocolate masses. To ensure consistency
145 in the rating of attributes, participants were trained during three sessions. They practiced rating maximum intensity of
146 each attribute using a sensation scale from 0 (not bitter/sweet/smooth) to 100 (extremely bitter/sweet/smooth).

147
148 During training sessions, participants consumed the reference sample $23_{Sc}\text{-}9_{Ho}$ and were instructed to rate its
149 maximum sensation at 50 for all attributes. The rating of sweetness and smoothness was practiced using defined
150 test samples (see Supplementary Information 6.3). The samples were tempered to $20 \pm 1^\circ\text{C}$ and served on plastic
151 trays with random three-digit codes. Each session was led by a sensory panel leader, a reference warm-up sample
152 was presented at the beginning of each session and the samples were presented in a balanced order. In addition, a
153 blind reference was included in the experimental design. Data from sample ratings was collected using EyeQuestion
154 (licensed to BFH-HAFL, Zollikofen, Switzerland).

155 2.4.2. Multiphase analysis

156 **Comparative Profiling:** Similar to comparing chocolate masses, all multiphase samples in experiment 1 ($Sw_{42_{Sc}\text{-}18_{Ho}}|_5$,
157 $Sw_{42_{Sc}\text{-}18_{Ho}}|_5$, $Sw_{42_{Sc}\text{-}0_{Ho}}|_3$, $Sw_{42_{Sc}\text{-}0_{Ho}}|_5$, $Sw_{23_{Sc}\text{-}0_{Ho}}|_3$, $Sw_{23_{Sc}\text{-}18_{Ho}}|_3$) were evaluated by comparative profiling. The same
158 panel rated the attributes on a unipolar scale from 0 to 100. In addition to rating maximum perception of the attributes
159 sweetness, smoothness and bitterness, the participants also rated overall perception of these attributes. After three
160 training sessions, the panel rated the samples twice across two sessions.

161
162 **Time-Intensity:** During three training sessions, participants were instructed on how to rate temporal sweetness
163 intensity. Specifically, they were taught to rate sweetness intensity at regular intervals of 0.1 Hz for the first thirty
164 seconds during consumption. Following this initial period, participants were permitted to continue rating the samples
165 at their own pace. To provide further guidance, participants were asked to rate the intensity when the sample had
166 completely melted (I_{melt}), as well as the final perceived sweetness sensation (I_{end}) at swallowing.

167
168 **Progressive Profiling:** Multiphase samples in experiment 2 (Ref (23_{Sc}-0_{Ho}), L_{42_{Sc}-0_{Ho}|2}, L_{42_{Sc}-0_{Ho}|6}, L_{42_{Sc}-0_{Ho}|12},
169 CiC_{42_{Sc}-0_{Ho}|2} and CiC_{04_{Sc}-0_{Ho}|2}), and Ref (23_{Sc}-9_{Ho})) were rated at three time points t_{start} , t_{max} , and t_{end} . Similar to comparative
170 profiling, participants were asked to rate sweetness sensation on a scale from 0 (not sweet) to 100 (extremely
171 sweet). Each session started with a warm-up sample of defined maximum sweetness intensity of 50. In addition to
172 assessing maximum sweetness intensity I_{max} , participants were instructed to rate initial (I_{start}) and final sweetness per-
173 ception (I_{end}), which was defined as the sensation before the last piece of sample had been completely swallowed. Due
174 to the pandemic, training and testing sessions were carried out at home under non-controlled atmosphere, and guided
175 via online sessions by a sensory panel leader. Data from both sensory evaluations were recorded using EyeQuestion
176 (licensed to BFH-HAFL, Zollikofen, Switzerland).

179 **2.5. Data Analysis**

180 **Single mass sensory and instrumental analysis:** In order to compare the ratings of the attributes (sweetness, smoothness and bitterness) among different single masses, multivariate comparison in RStudio was performed
181 (2023.03.0 Build 386, Posit Software, PBC). Attributes were set as dependent variables in a linear mixed-effect model
182 (lme4 library, lmer test library). Since each of the samples was uniquely described by sample code (e.g., 23_{Sc}-9_{Ho})
183 or the fixed factors hazelnut oil content (0,9 and 18 %w/w) and sugar content (4, 23 and 42 %w/w). Either sample
184 code or oil content and sugar content were set as fixed factors. Interaction between sessions and sequence of order
185 was treated as a linear fixed effect. In addition, prediction of the attributes was complemented by an intercept and a
186 random error for the intercept by grouping participants (11 participants). To check whether residuals of the models
187 were normally distributed, a residual simulation was performed using the DHARMA package. For significant results
188 with $p < 0.05$, a pairwise comparison (emmeans library) was performed with a Tukey post-hoc test.
189

190 As with the sensory data, instrumental data (calorimetry, rheology and particle size) were analyzed using a linear
191 mixed effects model. The data were previously grouped in two batches (=sessions) with three replicates per batch,
192 corresponding to all the masses produced for each of the sensory tests and instrumental analysis. Different measurement
193 variables, such as d₉₀, were designated as dependent variables. Meanwhile, oil, sugar content or sample ID,
194 were set as fixed factors. An intercept was included with the batches serving as random error. Similar to sensory analysis,
195 model normality was checked with the DHARMA package and significant results were analyzed with a post-hoc
196 Tukey test (emmeans library).

197 Different measurement variables, such as d₉₀, were designated as dependent variables. Meanwhile, oil and sugar
198 content, as well as sample ID, were set as fixed factors. An intercept was included with the batches serving as a
199 random error.

200 To investigate correlations between sensory and instrumental variables, a multicomparsion nonparametric Spearman
201 correlation plot was designed (library ggstatsplot, psych, Hmisc). Significant pairwise interactions were tested
202 with an unpaired Wilcoxon t-test (library ggstatsplot, psych, Hmisc).

203 **Multiphase comparative profiling:** As for single masses profiling, statistical analysis was performed with a
204 multivariate comparison in RStudio (2023.03.0 Build 386, Posit Software, PBC). The attributes smoothness, sweet-
205 ness and bitterness (maximum and total) were set as dependant variables, while sugar and hazelnut oil content of the
206 tongue-proximal layer were set as independent variables. In addition, the number of layers was included in the linear
207 model as an independent factor. Similar to single mass sensory, session and order were treated as a liner fixed effect
208 and the participants were set as random error. Significant results ($p < 0.05$) were compared using a Tukey post-hoc test.
209

210 **Multiphase time intensity:** Temporal sweetness intensity data were averaged across all participants for the two
211 test sessions, based on normalization of individual curves for both intensity and time. Time and intensity correction
212 is based on [18] and was slightly adapted to allow normalization for an ascent, plateau, and descent phase. A detailed
213 normalization and averaging procedure can be found in Supplementary Information 6.4. A number of key values
214 (e.g., time to peak or baseline intensity) were further analysed using a one-way analysis of variance with sweetness
215 intensity or time set as dependant variable. Samples, participants and sessions were treated as fixed factors. Tukey
216 was employed as a post-hoc test to further compare the means of the key values. Normalization and averaging method
217 was performed with a python script (Jupyter pyi version 3.6.3), and statistical analysis was conducted with Origin Pro
218 (version 2021).

219 **Multiphase progressive profiling:** During progressive profiling, sweetness intensity I_{start}, I_{max}, and I_{end} were de-
220 fined as dependent variables. Session and order were treated as a liner fixed effect and participants were set as random
221 error. Significant results ($p < 0.05$) were compared with a Tukey post-hoc test.
222

227 **3. Results and Discussion**

228 **3.1. Chocolate Mass Analysis**

229 **3.1.1. Instrumental Analysis**

230 This research centered on investigating the impact of inhomogeneously distributed sucrose at different spatial configurations on the perception of different attributes. To solely focus on the relationship of locally distributed sucrose on perception, chocolate masses were manufactured that share similar techno-functional characteristics. Such a design minimized potential interference of somatosensory confounders on taste perception [67, 17]. With this focus, sucrose was partially replaced with inulin and polydextrose. These agents were chosen specifically for their bulking properties [4, 21, 2]. All chocolate masses with varying hazelnut oil (*Ho*) content and sugar content (*Sc*) were characterized with laser diffraction to characterize particle sizes, rheology to provide information about flow properties, and calorimetry to quantify melting properties.

238

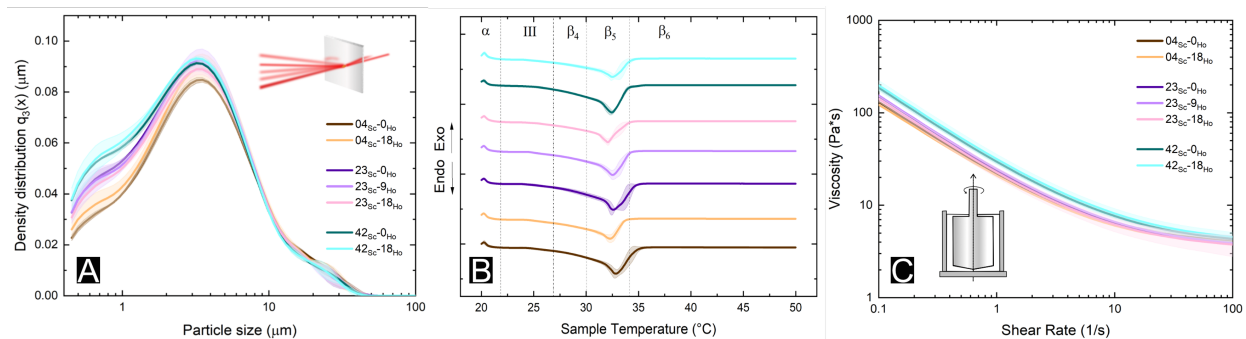


Figure 2: Instrumental analysis of all chocolate masses that varied in sucrose load (*Sc*) and/or hazelnut oil content (*Ho*). (A) Particle size distribution, (B) DSC curves with α and β indicating polymorphic crystals. Dashed lines separate their respective melting domains [20]. (C) Rheological flow curves. Standard deviation for all samples is colored around the mean values for (A)-(C).

239 After seven hours of grinding, all chocolate masses exhibited a monotonic size distribution pattern with a d_{90}
240 value below 30 μm, as shown in Figure 2A. This size reduction was essential, as particles below 30 μm are necessary
241 to avoid a gritty texture [6, 58], unaffected by composition. Thus, there was no observable effect on particle size due
242 to the type of bulking agent (e.g., F(2,7)[d_{90}] = 0.34, NS) or *Ho* content (F(2,7)[d_{90}] = 0.24, NS).

243
244 The flow curves depicted in Figure 2C showed non-Newtonian pseudoplastic behaviour, typical for chocolate [5, 31, 46]. Given their known impact on textural sensory perception, viscosity at shear rates of 10, 20, and 50 1/s
245 were specifically compared [14, 57, 65]. The data indicate a reciprocal relationship between sucrose load and viscosity
246 that is independent of shear rate, though significant deviations were observed only at a shear rate of 10 1/s ($p < 0.05$
247 for η_{10}) (detailed data available in the Supplementary Information 6.5). Contrary to Aidoo et al. [2, 3], the results
248 indicate that the lower bed density of sugar crystals compared to sugar replacers could be contributing to the observed
249 differences. This is probably due to shape differences between sugar crystals and amorphous inulin/polydextrose
250 spheres. While milling primarily determined particle breakage pattern, *Ho* content (e.g., F(2,7)[η_{10}] = 2.07, NS) and
251 *Sc* had only a minor influence on particle size distribution and, consequently, on the flow curves.

252
253 Regardless of *Ho* content or *Sc*, a single endothermic transition was registered between 25.2 °C (T_{onset}) and 34.9 °C
254 (T_{offset}), with melting peaks at 32 - 33 °C. This behavior aligns with the expectation for well-tempered chocolate [66].
255 Given the similarity in triacylglycerols (TAG) [61], notably their chain length, to those in cacao butter and the low
256 *Ho* contents (0-6.25 %w/w) used in this study, a similar crystallization behavior irrespective of *Ho* content is ex-
257 pected [59]. This similarity suggest that all chocolate masses would exhibit sensory characteristics associated with
258 well-tempered chocolate [1, 41]. Although cacao butter substitution had a considerable effect on several calorimetric
259 aspects, melting enthalpy was most strongly affected ($F(2,7) = 378.82$, $p < 2e-16$). Specifically, melting enthalpy, that
260 is the quantity of latent heat absorbed during melting, declined from about 44 - 45 J/g in pure chocolate to 35-37 J/g
261 is the quantity of latent heat absorbed during melting, declined from about 44 - 45 J/g in pure chocolate to 35-37 J/g

in chocolate blends with 6.25 %w/w Ho (see Supplementary Information 6.5). No effect of sugar substitution was observed on the melting characteristics (e.g., $F(2,7)[\text{melting enthalpy}] = 1.93, \text{NS}$), as detailed in the Supplementary Information 6.5.

265

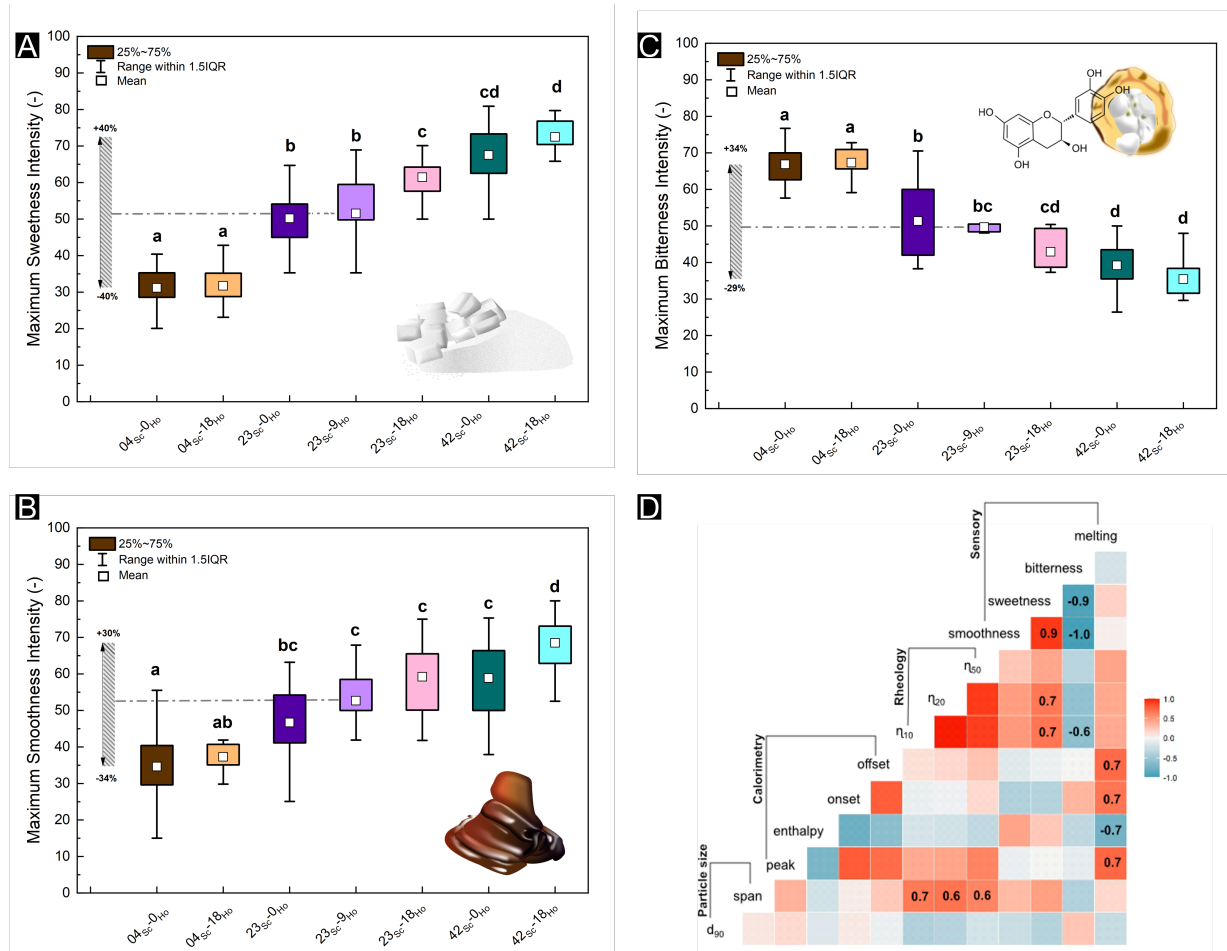


Figure 3: Sensory properties of chocolate masses with differences in hazelnut oil (Ho) content or sucrose (Sc) load. (A) Represents sweetness intensity, (B) denotes smoothness, and (C) shows bitterness evaluation. To the left of each plot, a range is introduced with written anchors to illustrate the degree of deviation from the reference sample. Mean intensity values sharing the same subscript do not significantly differ ($p < 0.05$). (D) Presents a correlation lookup table comparing sensory evaluations to instrumental chocolate mass characteristics. Only the most relevant and significant correlations are displayed for ease of visualization.

3.1.2. Sensory Analysis

This study employed comparative profiling to analyze the effects of Sc and Ho content on perceived sweetness, bitterness, and smoothness of chocolate masses. Findings revealed that increasing Sc intensified perceived sweetness ($F(2,98) = 240, p < 2e-16$), and intriguingly, substituting cacao butter with Ho also significantly elevated sweetness scores ($F(2,98) = 10, p < 2e-4$). Despite a nearly two-fold increase in sugar content in sample $42_{Sc}-0_{Ho}$ compared to $23_{Sc}-18_{Ho}$, no difference in perceived sweetness was reported, likely due to the inclusion of Ho . The potential mechanisms contributing to this increase in sweetness perception due to Ho addition are discussed below.

273

A higher Ho content led to a decrease in melting enthalpy and a reduced consumption time (see Figure 3D, $R^2 = -0.7$). Thereby, sucrose mass transfer was possibly accelerated, increasing sucrose concentrations at the tongue-

receptor level. To gain a deeper understanding of those effects, particularly the influence of Ho on the kinetics of sucrose release and the subsequent impact on sweetness perception, two cubical systems composed of 70 %w/w fat and 30 %w/w sugar were further examined. These samples, which differed in fat composition — either pure cacao butter or a blend of cacao butter and Ho (comprising 18 % of the total fat, similar to the oil to fat ratio in the high Ho samples) — were evaluated by ten panelists over a duration of 45 seconds, after which they were expectorated. The post-tasting expectorate was analyzed to determine salivary flow rate and sucrose concentration. Detailed methodology can be found in the Supplementary Information 6.6. Approximately, an 150 % increase of aqueous sucrose concentration in the aqueous bolus was observed when the ratio of cacao butter was reduced, as measured by refractometry. While in-saliva sugar content was strongly influenced by melting enthalpy, salivary flow was not significantly different between both samples. This suggests that replacing cacao butter with Ho exerted a pronounced physico-chemical influence on perception.

Moreover, an interplay between sweetness perception and smoothness scores was observed (Figure 3A, B and D, $R^2 = 0.9$). However, viscosity of melted chocolate did not fully explain smoothness scores (e.g., $R^2 = 0.3$ for η_{50}), prompting further investigation into the role of friction in textural sensory perception. Interestingly, own measurements show that at high sugar loads friction was found to be increased, contradicting the typically anticipated inverse relationship between smoothness and friction [36]. Method and results are detailed in Supplementary Information 6.7. This could be attributed to the aggregation of sugar particles in a lipid phase at low shear rates. These results imply that textural differences might be influencing taste perception more perceptually than physicochemically.

As for bitterness, primarily elicited by flavan-3-ols in cocoa solids [44, 15], it was strongest perceived at low sucrose contents due to the absence of the well-documented masking effect [25]. A significant inverse relationship between Ho content and bitterness was observed ($F(2,98) = 5$, $p < 7e-3$), especially evident in samples with intermediate Sc . This suppression of bitterness was most effective where neither sweetness nor bitterness dominated perception. However, this phenomenon requires further investigation as the extent of this effect varies across different studies [56, 37].

These findings open up the possibility of enhancing sweetness perception without increasing sugar content, suggesting the relevance of potential physicochemical and perceptual mechanisms underlying these sensory perceptions.

3.2. Multiphase analysis

Our findings highlight the importance of high sucrose concentrations located near the tongue in initiating sweetness sensations. As shown in Figure 5, sample $CiC_{42_{Sc}-0_{Ho}} I_2$ was perceived 31 % sweeter than sample $CiC_{04_{Sc}-0_{Ho}} I_2$, indicating that concentration of tastants, such as sucrose, near taste receptors is key to strong taste perception [47, 23, 38]. Notably, in fat-continuous samples, a 10-second delay between consumption and taste perception was observed. This delay is linked to the sequence of processes needed for sucrose to interact with the oral epithelium, which involves cacao butter melting [63]. The pace of this phase change is governed by melting enthalpy, with higher Ho contents facilitating quicker transitions from solid to liquid and consequently making sucrose quicker available (see Figure 4D for I_{start} , Figure 2B and Supplementary Information 6.5). As consumption progressed, the impact of Ho content and Sc on sweetness perception attenuated (see Figure 4F). Nonetheless, sample $L_{23_{Sc}-18_{I_8}} I_3$ was still perceived 11% sweeter than the reference (see Figure 4A).

While a clear correlation between sweetness, bitterness and smoothness was evident for single masses, no such trend was observed in multiphase systems, as detailed in Figure 4B-C. Alternatively, numerous studies have underscored the fact that sweetness perception is not only influenced by the quantity of sweet substances, but also by the delivery pattern of these stimuli [8, 9, 11, 10, 29, 50, 48, 49, 33, 34, 7]. Specifically, a discontinuous presentation of alternating sweetness levels has been shown to modify perceived intensity of sweetness. However, our findings suggest that alterations in Ho content alone can amplify sweetness perception, even in the absence of difference in sweetness levels of chocolate masses. As evidenced in Figure 4A, sample $L_{23_{Sc}-18_{I_8}} I_3$ elicited 15% greater sweetness compared to sample $L_{23_{Sc}-0_{I_8}} I_3$. This finding points to the potential role of various mechanisms, such as physicochemical, pre-conscious, and cognitive processes, colloquially summarized as pulsatile stimulation.

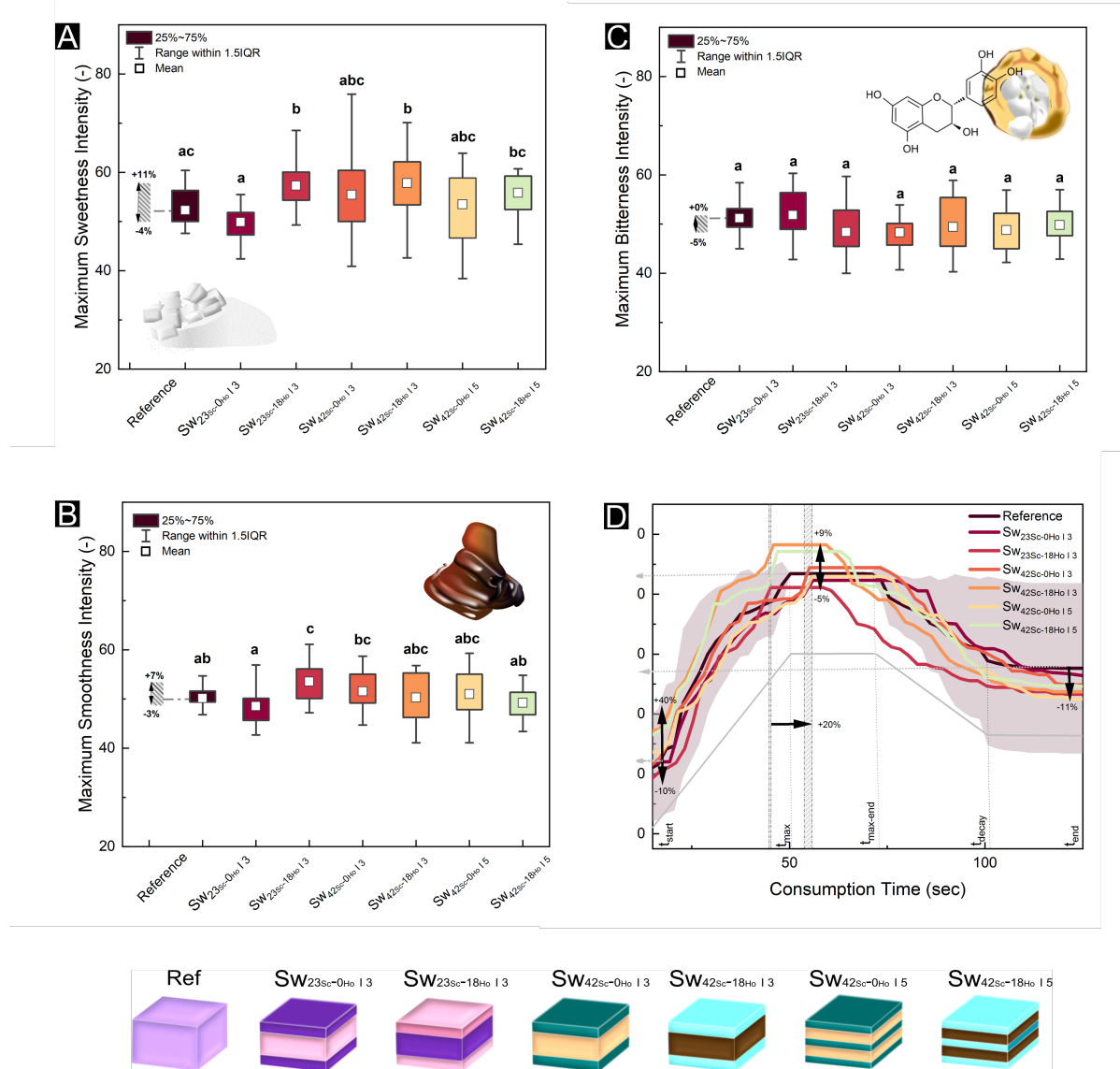


Figure 4: Sensory properties of multiphase samples assessed during Experiment 1. (A) Refers to sweetness intensity, (B) to smoothness, and (C) to bitterness. To the left of each plot, a range is introduced with written anchors to illustrate the degree of deviation from the reference sample ($SW_{23Sc-0Ho}$). Mean intensity values with the same subscript are statistically indistinguishable ($p < 0.05$). (D) Temporal evolution of sweetness, as assessed through time-intensity measurements. Like with the single masses, arrows at the beginning ($I_{start,Ref}$), at the peak ($I_{max,Ref}$), and at the end ($I_{end,Ref}$) of the plot depict the dimension of deviations from the homogeneous reference at different points in time. The temporal regime is divided into three stages: onset, maximum plateau, and decay. It is shown for the reference sample in grey lines below the sample time-intensity curves. Furthermore, the horizontal arrow indicates the delay in peak intensity onset produced by the substitution of Ho in the tongue-proximal layer. The standard deviation for the reference sample is shown as an example.

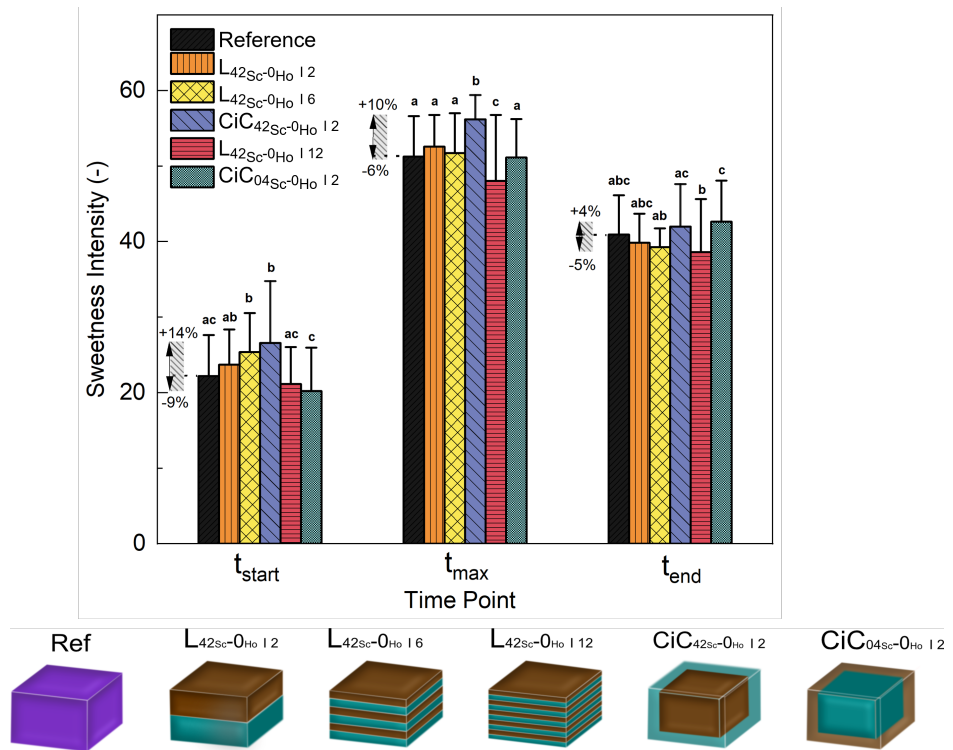


Figure 5: Mean sweetness intensity ratings of all samples tested during Experiment 2 at three time points t_{start} , t_{\max} and t_{end} . To the left of each plot, a range is introduced with written anchors to illustrate the degree of deviation from the reference sample. Mean intensity values with the same subscript are statistically indistinguishable ($p < 0.05$).

326 One theory to explain this phenomenon draws on the “Brück-Bartley effect” from vision science, where a flick-
327 ering stimulus appears brighter than a continuous one [70]. Similarly, rodents exposed to high-frequency pulsatile
328 taste stimuli were reported to perceive an increased magnitude of taste [26, 28]. However, in the context of semi-solid
329 food consumption, it’s unlikely for such high-frequency stimuli to occur - for instance, a frequency of approximately
330 every 5 seconds as employed by Burseg et al. [8] in experiments with liquid samples. An alternative explanation
331 might be that alternation between high and low sucrose concentrations results in reduced taste adaptation [27, 64, 12].
332 Nonetheless, when comparing samples $L_{42Sc-0Ho} 12$ and $L_{42Sc-0Ho} 112$, the increase in number of pulses (from 2 to 12) did
333 not result in an increased sweetness perception. More probable, adaptation to the stimuli occurred for all samples,
334 as the frequency of pulses was too low or, because “pulses” merged at later stages to a uniform signal. This was
335 corroborated by the absence of a layer effect on sweetness perception in experiment 1 ($F(2,85) = 1.5009, p = 0.22$).

336
337 The most likely explanation for pulsatile stimulation in semi-solid food centers around the influence of expecta-
338 tion. Expectations, whether prompted by text or taste, can modulate both cortical responses and sensory perception of
339 taste [24, 51, 60, 55, 69]. For example, a study by Wilton et al. [68] found that when participants were presented with
340 conflicting cues, they rated low-sweet solutions as significantly sweeter (by over 250 %). This finding strengthens the
341 argument that early perception of sweet taste can be influenced by expectations. Considering these research findings,
342 we suggest that a shift in context, triggered by an initial sweet stimulus, can significantly impact the overall taste
343 assessment [39]. This phenomenon, sometimes referred to as bias [42, 43], suggests that the first impression of sweet-
344 ness could be stored at a pre-conscious level to be further integrated into perception. This idea is supported by our
345 data and could be seen in Figure 4A, which emphasizes the importance of the first layer of hazelnut oil ($F(2,98) = 5,$
346 $p < 0.01$) in coding maximum and overall sweetness perception.

347
348 In summary, our study suggests that differences in sweetness perception through pulsatile stimulation are mainly
349 due to a contextual shift triggered by the initial taste sensation.

350 **4. Conclusion**

351 This research examined the interplay between perceived sweetness and spatial distribution of bulking agents and
352 fat in chocolate structures. In this regard, we developed chocolate masses varying in sugar or hazelnut oil content, a
353 change that impacted melting properties but otherwise left the techno-functional characteristics unaltered. This was
354 key to unambiguously link the effects of structural anisotropy to sweetness perception. The substitution of sugar with
355 a mixture of inulin/polydextrose had only minimal impact on chocolate properties, such as particle size distribution,
356 flow, and melting behavior. In contrast, replacing cacao butter with hazelnut oil not only decreased melting enthalpy
357 and consequently melting time, but also led to a noticeable increase in perceived sweetness. The latter was confirmed
358 by sensory tests, implying a significant role for hazelnut oil in enhancing sweetness. In-vivo tests propose that this
359 sweetness augmentation could partially be due to accelerated sucrose release into saliva when melting enthalpy is
360 reduced. However, we found no clear correlation in the rheology and tribology data that could explain the smoothness
361 sensation closely associated with sweetness perception. We, therefore, hypothesize that the perception of this texture
362 attribute is not strictly physical but likely integrated with sweetness perception at a cognitive level.

363
364 For layered samples, sensory data indicated that sweetness perception diverged by -4 % to +11 % compared to a
365 homogeneous reference. Notably, sweetness perception was highest in samples with layers differing only in hazelnut
366 oil content. This challenges previous studies that underscored the necessity of sugar gradients to enhance sweetness
367 perception. Another key finding was observed in experimental series 2, where panelists perceived augmented sweet-
368 ness only when initially exposed to layers high in sugar, as demonstrated in the cube-in-cube systems. This supports
369 the conceptual idea that initial taste perception can create a perceptual baseline for overall sensory experience. How-
370 ever, increasing complexity, as done from 2-layered to 12-layered structures, did not enhance sweetness. This implies
371 that structural intricacy may not be as important for modifying sweetness perception.

372
373 Our research highlights the potential to manipulate sweetness perception through spatial modifications. This
374 approach involves altering release kinetics by modifying the fat phase and by tailoring structures using additive man-
375 ufacturing. This strategy is particularly compelling as it paves the way for innovative sugar reduction techniques
376 without sacrificing sensory experience. In conclusion, our study provides insights into the influence of structural com-
377 position on taste perception, particularly sweetness. Furthermore, it underscores the exciting potential that precision
378 food manufacturing holds for the future of sensory experiences in food consumption.

379 **5. Acknowledgements**

380 The authors thank the Swiss National Science Foundation and Innosuisse for funding of the Bridge Project (No.
381 20B2-1-180971/1). We thank Daniel Kiechl for his help with installing the setup.

³⁸² **6. Supplementary Information**

³⁸³ **6.1. Printer Settings**

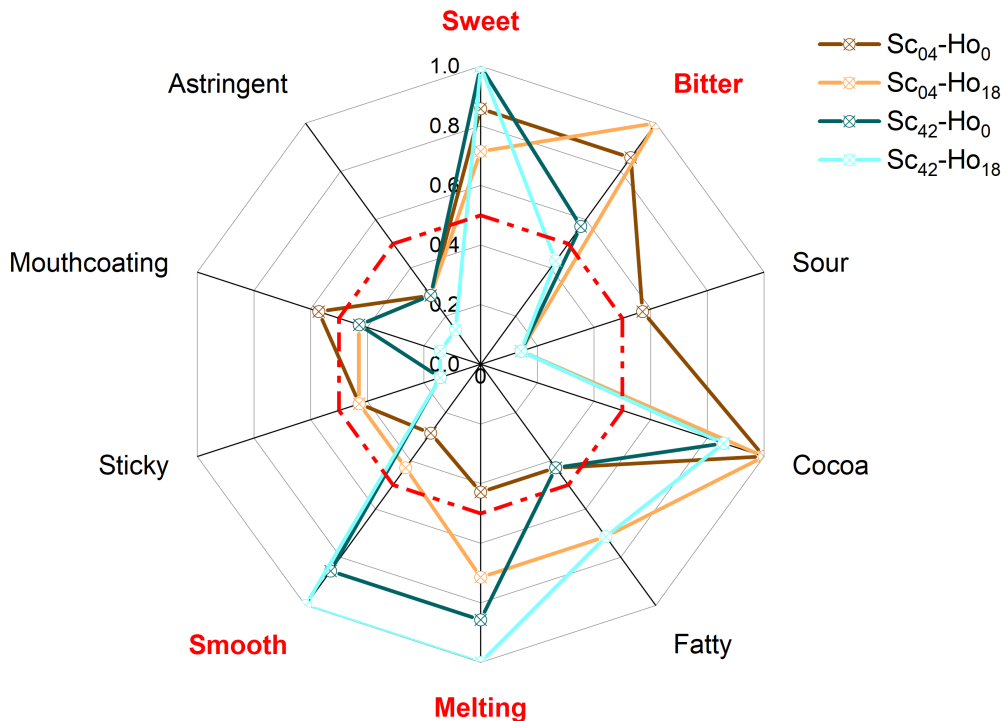
³⁸⁴ Detail settings of printer and firmware settings considered for the manufacturing of the multiphase systems.

Supplementary Table 1: Printer Firmware Settings (EEPROM).

Firmware Settings	Extruder 1	Extruder 2
X-Axis (steps/mm)	266	266
Y-Axis (steps/mm)	266	266
Z-Axis (steps/mm)	1000	1000
X-Axis acceleration (mm/s ²)	1000	1000
Y-Axis acceleration (mm/s ²)	1000	1000
Z.Axis acceleration (mm/s ²)	100	100
Extr X-Offset (steps)	0	32000
Extr Y-Offset (steps)	0	200

Supplementary Table 2: Printer Settings.

Printer Settings	Extruder 1/2
Nozzle diameter (mm)	0.8)
Layer height (mm)	0.8
First layer height (mm)	0.8
Vertical shell perimeter (-)	1
Horizontal shell top (-)	1
Horizontal shell bottom (-)	1
Seam position	Nearest
Fill density (%)	100
Fill pattern	Concentric
Top/Bottom fill pattern	Rectilinear
Skirt	Each phase change
Skirt loops (-)	2
Skirt distance from object (mm)	10



Supplementary Figure 1: Check-All-That-Applies data generated from the evaluation of four chocolate masses identified as $04_{Sc}-0_{Ho}$, $04_{Sc}-18_{Ho}$, $42_{Sc}-0_{Ho}$, and $42_{Sc}-18_{Ho}$. The red dotted line demarcates a 50 % selection threshold among panelists. Attributes highlighted in red were chosen for further sensory analysis based on their significant proportion of selection and notable differences observed during preliminary tests.

³⁸⁵ 6.2. Check-All-That-Applies

³⁸⁶ Participants conducted a Check-All-That-Apply (CATA) test to describe the sensory profiles of four selected
³⁸⁷ chocolate masses ($04_{Sc}-0_{Ho}$, $04_{Sc}-18_{Ho}$, $42_{Sc}-0_{Ho}$ and $42_{Sc}-18_{Ho}$). They were presented with a list of ten pre-defined
³⁸⁸ attributes to select attributes for each sample. The overview of the data is presented in Supplementary Figure 1.

³⁸⁹ **6.3. Attribute Calibration for Sensory**

³⁹⁰ Before the evaluation of bitterness, sweetness, and smoothness, a range of anchor points was set to calibrate the
³⁹¹ scales for smoothness and sweetness, with values ranging from 0 to 100. The reference probe, designated as $23_{Sc}\text{-}09_{Ho}$,
³⁹² was assigned a midpoint value of 50 on each scale (bitterness, sweetness, and smoothness). This calibration process
³⁹³ involved reconstituting sucrose in tap water at concentrations outlined in Supplementary Table 3. The relationship
³⁹⁴ between the defined sucrose load and sweetness intensity, as pre-tested and adapted from Karalus et al. (2016) [32],
³⁹⁵ was employed. Additionally, anchor points for smoothness were calibrated by adjusting the conching time from 1.5 to
³⁹⁶ 12 hours and by including chocolate masses with higher Ho contents at higher smoothness ratings (see Supplementary
³⁹⁷ Table 4). During the panel's training for single and multiphase masses, calibration for both smoothness and sweetness
³⁹⁸ was practiced.

Supplementary Table 3: Calibration standards for sweetness intensity during comparative profiling testing.

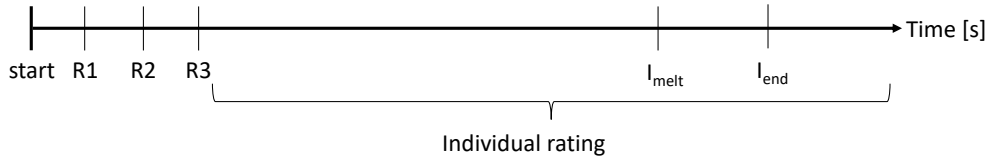
Terminology	Sucrose concentration	Sweetness rating
slightly less	30	20
little less	40	35
reference	50	50
little more	60	65
slightly more	70	80

Supplementary Table 4: Calibration standards for smoothness intensity during comparative profiling testing.

Chocolate Masses	Conching time	Smoothness rating
$23_{Sc}\text{-}0_{Ho}$	1.5	10
$23_{Sc}\text{-}0_{Ho}$	7	40
$23_{Sc}\text{-}9_{Ho}$	7	50
$23_{Sc}\text{-}18_{Ho}$	7	60
$23_{Sc}\text{-}18_{Ho}$	12	75

399 *6.4. Time-Intensity Methodology*

400 In Temporal Intensity (TI) measurements, sweetness was analyzed. Panelists evaluated a total of seven chocolate
401 multiphase systems, comprising one single-phase reference and six multi-phase systems. The tasting protocol was
402 consistent with comparative profiling, and panelists were tasked with rating sweetness intensity every ten seconds for
403 the first three ratings (R1, R2, R3). Beyond this point, panelists could choose their rating frequency. However, two
404 additional fixed rating points were established: I_{melt} , the point at which the sample was entirely melted, and I_{end} , the
405 rating immediately prior to swallowing (Supplementary Figure 2).



Supplementary Figure 2: Illustration of the rating method in TI. The three first ratings are recorded after 10, 20 and 30 seconds (R1, R2, R3), followed by an individual rating. I_{melt} and I_{end} are two other fixed rating points and recorded when the sample is completely molten (I_{melt}) and before swallowing (I_{end}).

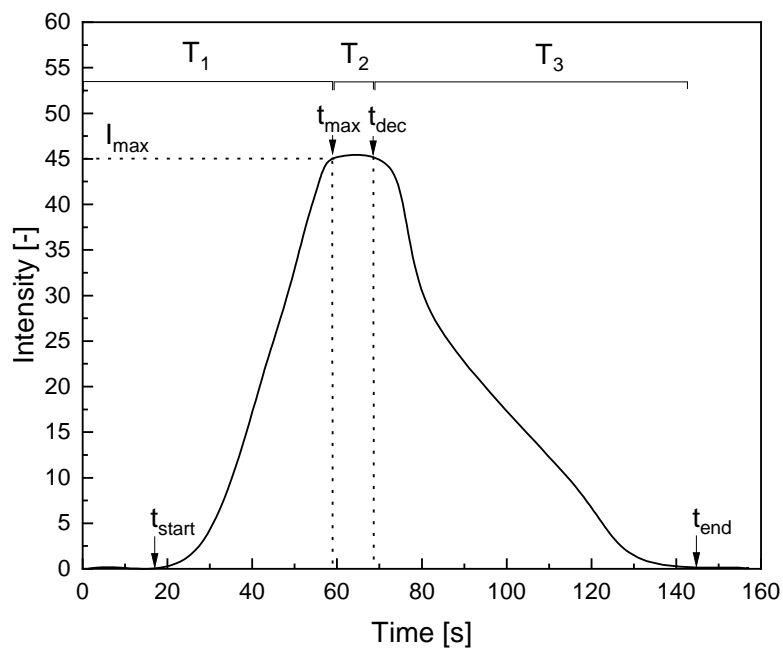
406 The method was exercised in three sessions and evaluated in another two sessions. For all sessions, the multi phase
 407 systems in experimental series 1 were sensorially evaluated. The obtained data was averaged, based on normalization
 408 of individual curves for both intensity and time. According to Equation 1, the individual dynamic intensity $I'(t)$
 409 correction is based on normalizing the individual intensity $I(t)$ with the ratio of overall maximum intensity I_{max,P_j} to
 410 $I_{max,i}$.

$$I(t)'_{P_j} = \frac{I_{max,P_j}}{I_{max,i}} * I(t) \quad (1)$$

411 To accommodate an x-axis normalization for non-monotonic curve shapes, simple averaging compared to intensity
 412 can lead to a loss in information about individual trends, especially from outliers or a minority pattern. Our method is
 413 based on the extension of [40], with some minor addendum. We are referring to the following parameters, describing
 414 all relevant parameters relevant for TI measurements:

- 415 • Maximum intensity (I_{max}): largest registered value for perceived intensity.
- 416 • Starting time (t_{start}): first value of time when intensity is greater than 0.
- 417 • Maximum time (t_{max}): the first time at which maximum intensity registered.
- 418 • Decline time ($t_{decline}$): the time at which the curve starts to decline from maximum intensity and the last time at
 419 which a maximum intensity is registered.
- 420 • Finish time (t_{end}): the time when the intensity first returns to 0, which is also called persistence time, or extinc-
 421 tion time.
- 422 • Recording time: from time set to 0 to end of recording.

423 In our procedure, next to I_{max} , four ‘time landmarks’ are averaged, namely starting time, time to maximum, time
 424 at which the curve starts to descend from I_{max} and ending time. The time normalization accommodates three different
 425 time domains (T_1, T_2, T_3), framed by the above listed landmarks (Supplementary Figure 3). The curves are then
 426 normalized in the t-direction to have the same $t_{start}, t_{max}, t_{decline}$, and t_{end} per product, according to the equation shown
 427 in Supplementary Figure 4.



Supplementary Figure 3: A typical TI curve with the plateau of maximum intensity and the three different time domains (T_1 , T_2 , T_3), adapted from Liu et al. (1990) [40].

428 If t_{decline} is equivalent to t_{max} , t' per product is reduced to the normalization of t' with the intervals (1) and (3). If
 429 I_{end} is non-zero, the curve is discarded. To average the values of I , each curve per product cluster is divided into n
 430 equal time intervals ($n = 60$) and arithmetically averaged as one master curve per product. The automatic averaging
 431 method was conducted with a Python script, loading the raw text files.

432 The obtained results for the landmarks were evaluated by a one-way analysis of variance (ANOVA) with sweetness
 433 intensity or the specific time as dependent variables. Samples, panellists and sessions were treated as fixed factors.
 434 Fisher's LSD was used for the comparison of means. All data analysis of the sensory tests was done with the integrated
 435 Origin analysis tool. Significance was defined as $p < 0.05$.

$$t' = \begin{cases} \frac{(t_{\text{max}} - t_{\text{start}})}{(t_{\text{max},i} - t_{\text{start},i})}(t - t_{\text{start},i}) + t_{\text{start}} \text{ when } t_{\text{start},i} \leq t \leq t_{\text{max},i} & (1) \\ \frac{(t_{\text{dec}} - t_{\text{max}})}{(t_{\text{dec},i} - t_{\text{max},i})}(t - t_{\text{max},i}) + t_{\text{max}} \text{ when } t_{\text{max},i} < t < t_{\text{dec},i} & (2) \\ \frac{(t_{\text{end}} - t_{\text{dec}})}{(t_{\text{end},i} - t_{\text{dec},i})}(t - t_{\text{dec},i}) + t_{\text{dec}} \text{ when } t_{\text{dec},i} \leq t \leq t_{\text{end},i} & (3) \end{cases}$$

Supplementary Figure 4: Equation to normalize the TI curves in t-direction.

436 *6.5. Instrumental Data - Results*

437 The following Supplementary Table 5 summarizes the means for each instrumental measurement method em-
438 ployed during analysis.

Supplementary Table 5: Summary of all chocolate masses, presented with their respective mean and standard deviation for each measurement method (particle size, rheology and calorimetry). The methods are further divided into specific numbers, used for comparisons among all masses. Certain numbers are accompanied by letters signifying significant differences: K for $p < 0.05$, K' for $p < 0.01$, and K'' for $p < 0.001$. The final three rows were created by grouping the sugar load (Sc) and hazelnut oil content (Ho) into factors for a linear mixed model. Significance between these factors was evaluated using a post-hoc Tukey test. The number of asterisks (*) represents different levels of significance (* < 0.5, ** < 0.1, *** < 0.01, **** < 0.001).

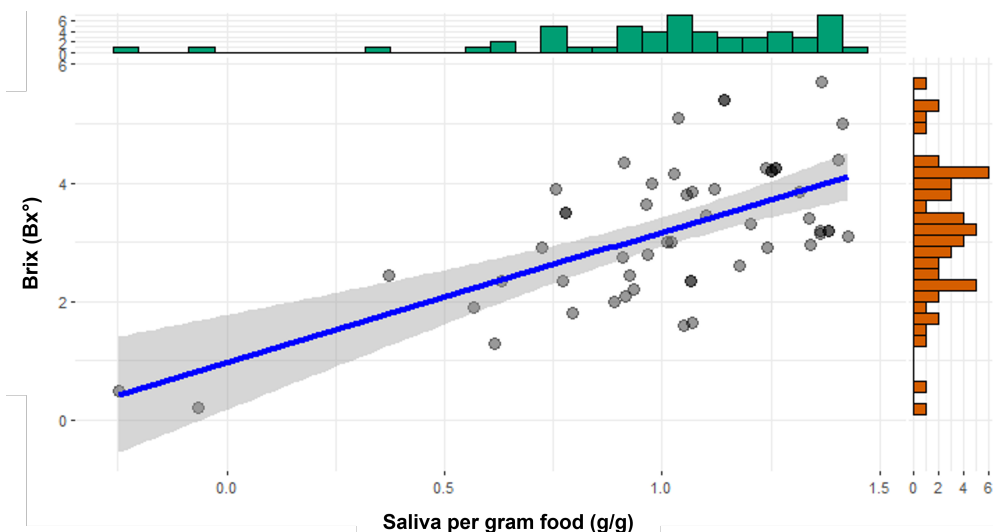
Chocolate Mass (Letter)	Particle Size Distribution		Rheology		Differential Scanning Calorimetry				
	Span (-)	d_{90} (μm)	$\eta_{10}(Pa * s)$	$\eta_{20}(Pa * s)$	Enthalpy (J/g)	Onset (°C)	Peak (°C)	Offset (°C)	
04 _{Sc} -0 _{Ho} (A)	3.1	29.3 ± 0.5	6.4 ± 0.4 ^F	5.2 ± 0.3	4.4 ± 0.3	-44.8 ± 1.7	26.3 ± 0.3	32.8 ± 0.5	34.6 ± 0.4
04 _{Sc} -18 _{Ho} (B)	2.9 ± 0.2	26.5 ± 3.2	5.6 ± 0.1	4.9	4.2	-37 ± 0.5 ^{A,C,D,F,F'}	25.3 ± 0.1 ^{B,D}	32.1 ± 0.4	33.8 ± 0.2 ^{K,C,F}
23 _{Sc} -0 _{Ho} (C)	3.1 ± 0.2	26.0 ± 2.0	6.4 ± 0.1	5.0	4.2 ± 0.1	-44.9 ± 1.1	26.2 ± 0.5	32.7 ± 0.4	34.6 ± 0.6 ^A
23 _{Sc} -9 _{Ho} (D)	2.3 ± 0.2	25.4 ± 2.4	6.3 ± 0.4 ^F	4.9 ± 0.5	4.2 ± 0.3	-41.2 ± 0.7 ^{A,C,D,F,F'}	25.7 ± 0.2 ^{E,G}	32.5 ± 0.4	34.3 ± 0.6
23 _{Sc} -18 _{Ho} (E)	3.2 ± 0.1	27.6 ± 1	6.6 ± 0.2 ^F	5.3 ± 0.2	4.3 ± 0.2	-35.3 ± 0.8 ^{A,C,D,F,F'}	25.1 ± 0.1 ^{A,K}	32.2 ± 0.4	34.1 ± 0.6
42 _{Sc} -0 _{Ho} (F)	3.24 ± 0.1	26.4 ± 0.3	7.8 ± 0.4	6.1 ± 0.3	4.9 ± 0.3	-44.7 ± 1.1	26.1 ± 0.6	32.8 ± 0.6	34.6 ± 0.6
42 _{Sc} -18 _{Ho} (G)	3.34.9 ± 0.1	27.0 ± 1.1	7.3 ± 0.5	5.7 ± 0.3	4.5 ± 0.2	-36.3 ± 1.1 ^{A,C,D,F,F'}	25.2 ± 0.3 ^K	32.2 ± 0.5	34 ± 0.2 ^A
Sugar load (Sc)	F(2,7) = 1.46 (NS)	F(2,7) = 0.34 (NS)	F(2,7) = 22.89 ***	F(2,7) = 11.83 ***	F(2,7) = 6.2 *	F(2,7) = 1.93 (NS)	F(2,7) = 1.73 (NS)	F(2,7) = 0.75 (NS)	F(2,7) = 0.28 (NS)
Hazelnut oil content (Ho)	F(2,7) = 0.25 (NS)	F(2,7) = 0.24 (NS)	F(2,7) = 2.07 (NS)	F(2,7) = 1.95 (NS)	F(2,7) = 1.47 (NS)	F(2,7) = 378.82 ***	F(2,7) = 68.93 ***	F(2,7) = 6.75 **	F(2,7) = 12.58 ***
Sc x Ho	F(2,7) = 0.52 (NS)	F(2,7) = 0.99 (NS)	F(2,7) = 0.29 (NS)	F(2,7) = 0.18 (NS)	F(2,7) = 0.56 (NS)	F(2,7) = 2.41 (NS)	F(2,7) = 0.75 (NS)	F(2,7) = 0.52 (NS)	F(2,7) = 0.67 (NS)

439 **6.6. Sucrose delivery quantification**

440 In this study, we investigated the impact of hazelnut oil content on the perceived sweetness of two distinct samples,
 441 differentiated solely by their hazelnut oil content. The samples (30 mm x 30 mm x 3 mm) comprised 70 % fat (either
 442 pure cocoa butter for sample 1 or an 18 %w/w hazelnut oil mix for sample 2), supplemented with 30 % powdered
 443 sugar. A non-cocoa based sample was selected to isolate and emphasize the effect of hazelnut oil on taste perception.
 444 Experiment 1 revealed an enhanced sweetness perception for the hazelnut oil-containing sample at medium sugar
 445 concentration levels. While a correlation between melting time and the amount of cocoa butter substitute was evident,
 446 it remained uncertain whether the perceived enhancement was due to somatosensation or an increased availability of
 447 sucrose at the receptor level.

448 To explore this, we designed an experiment involving ten panelists, each instructed to lick a sample for 45 seconds
 449 after their tongue was rinsed and cleared of any residue. The licked samples were subsequently collected, diluted, and
 450 centrifuged until a clear supernatant was achieved. Sugar content in the water phase was estimated using a refractometer
 451 (LLG-uniREFRACTO 5, Lab Logistics Group GmbH, Germany), from which the theoretical melted fraction was
 452 derived. An overview of the workflow is visualized in Supplementary Figure 6. In addition, a pairwise assessment was
 453 conducted, where panelists were asked to evaluate which sample was sweeter. The presentation order was balanced,
 454 and each panelist completed three pairwise evaluations. The sensory data were analysed with the sensR package.

455 Supplementary Table 6 provides a summary of the collected data. As anticipated, participants consistently rated
 456 sample 2 as sweeter in pairwise comparisons. Despite the lack of a significant difference in the saliva content per
 457 gram of food between the two samples ($p = 0.35$), Supplementary Figure 5 depicts a clear trend towards a higher Brix
 458 content correlating with increased saliva content ($R^2 = 0.63$). In contrast, a substantial increase in the sugar content of
 459 saliva was observed, with an increase factor of over 150 %, indicating a notable physicochemical correlation between
 460 the heightened sweetness perception in samples with added hazelnut oil.



Supplementary Figure 5: Correlation plot showing the relationship between saliva per gram of food (g/g) and the Brix content ($^{\circ}\text{Bx}$) in the aqueous phase. The top and right side of the plot present histograms indicating the frequency distribution of respective values along both axes. The blue line in the plot depicts the regression line, while the surrounding grey shade signifies the 95 % confidence interval.

Supplementary Table 6: Summary of results obtained from sucrose delivery measurements including the amount of saliva per food, the measured Brix content ($^{\circ}$) and the proportion of selections from paired comparisons. For the amount of saliva and brix content, a t-test test was conducted. For sensory analysis, the data were evaluated binomially. The number of asterisks (*) represents different levels of significance (* < 0.5 , ** < 0.1 , *** < 0.01 , **** < 0.001).

Sample	g Saliva/g Food (g/g)	Brix content ($^{\circ}$)	Ratio of selections in paired comparisons (-)
1 - w/o HNO	0.95 ± 0.41	2.54 ± 1.03	100 %
2 - w/ HNO	1.05 ± 0.25	3.87 ± 0.89****	0 %****

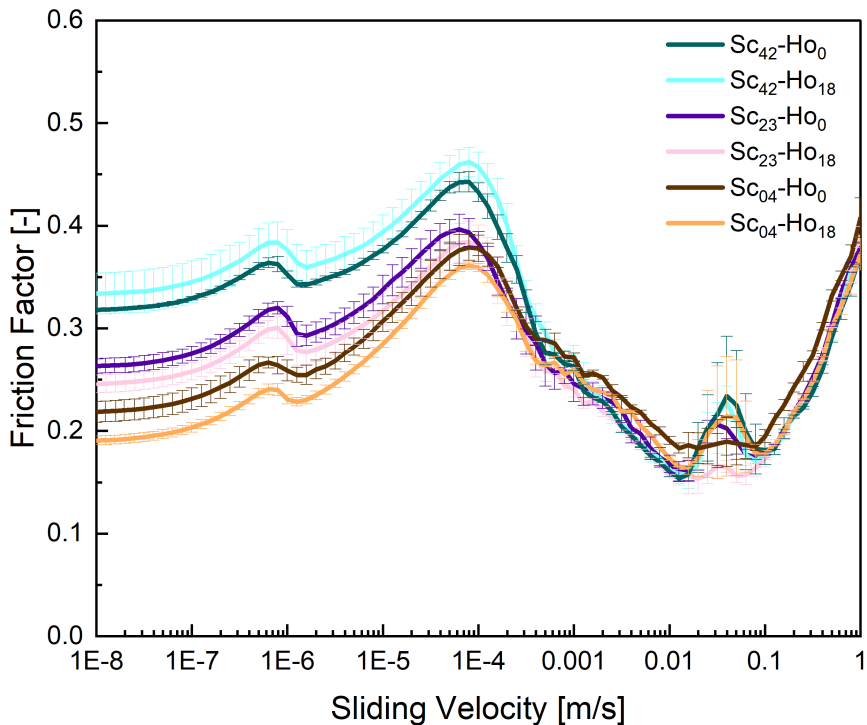


Supplementary Figure 6: Workflow for in-vivo quantification of sugar content.

463 6.7. Tribology measurements

464 All chocolate samples underwent analysis using an Anton Paar MCR702 MultiDrive rheometer, equipped with a
 465 Ball on Three Pins (BTP) tribology cell and a CTD180 temperature control element (all Anton Paar GmbH, Austria).
 466 A 0.127 m diameter glass ball (BC12.7, Anton Paar GmbH, Austria) and three smooth, hydrophobic polydimethyl-
 467 siloxane (PDMS) pins (SylgardTM 184 silicone elastomer, base and curing agents, Dow Corning, USA) served as
 468 tribology surfaces. The molten chocolate samples were carefully transferred into the tribology cell using a metal
 469 spoon.

470 Measurements began after the sample temperature was maintained at 35 °C for 30 minutes. All chocolate masses
 471 were analyzed under normal forces of $F_{N,tribo} = 1$ N. The friction force was measured against sliding velocity, ranging
 472 from 10^{-8} m/s to 1 m/s. Pure cocoa butter was assessed as a reference. Each sample underwent ten consecutive
 473 measurements with alternating increasing and decreasing speed ramps. The initial two repeats were excluded due
 474 to substantial deviation from subsequent runs. The average and standard deviation from the next four runs were
 475 calculated for both ramp up and ramp down and were used to derive the Stribeck curve. The increasing velocity ramp
 476 Stribeck curves were used for evaluation. Post-measurement, each sample was removed and the upper and lower
 477 geometries were thoroughly cleaned with hot water and standard cleaning agent.
 478



Supplementary Figure 7: Stribeck curves of chocolate masses $04_{Sc}-0_{Ho}$, $04_{Sc}-18_{Ho}$, $23_{Sc}-0_{Ho}$, $23_{Sc}-18_{Ho}$, $42_{Sc}-0_{Ho}$, and $42_{Sc}-18_{Ho}$, obtained at 35 °C and $F_{N,tribo} = 1$ N with a BTP geometry.

479 References

- 480 [1] Afoakwa, E. O., Paterson, A., and Fowler, M. (2008). Effects of particle size distribution and composition on rheological properties of dark
481 chocolate. *European Food Research and Technology*, 226(6):1259–1268.
- 482 [2] Aidoo, R. P., Appah, E., Van Dewalle, D., Afoakwa, E. O., and Dewettinck, K. (2017). Functionality of inulin and polydextrose as sucrose
483 replacers in sugar-free dark chocolate manufacture – effect of fat content and bulk mixture concentration on rheological, mechanical and melting
484 properties. *International Journal of Food Science and Technology*, 52(1):282–290.
- 485 [3] Aidoo, R. P., Clercq, N. D., Afoakwa, E. O., and Dewettinck, K. (2014). Optimisation of processing conditions and rheological properties
486 using stephan mixer as conche in small-scale chocolate processing. *International Journal of Food Science and Technology*, 49(3):740–746.
- 487 [4] Aidoo, R. P., Depypere, F., Afoakwa, E. O., and Dewettinck, K. (2013). Industrial manufacture of sugar-free chocolates - Applicability of
488 alternative sweeteners and carbohydrate polymers as raw materials in product development. *Trends in Food Science and Technology*, 32(2):84–
489 96.
- 490 [5] Beckett, S., Fowler, M., and Ziegler, G. R. (2017). *Beckett's Industrial Chocolate Manufacture and Use*.
- 491 [6] Breen, S. P., Etter, N. M., Ziegler, G. R., and Hayes, J. E. (2019). Oral somatosensory acuity is related to particle size perception in chocolate.
492 *Scientific Reports*, 9(1):1–10.
- 493 [7] Burkard, J., Nain Shah, A., Harms, E., and Denkel, C. (2023). Impact of spatial distribution on the sensory properties of multiphase 3D-printed
494 food configurations. *Food Quality and Preference*, 108(December 2022):104850.
- 495 [8] Burseg, K. M. M., Brattinga, C., de Kok, P. M. T., and Bult, J. H. F. (2010a). Sweet taste enhancement through pulsatile stimulation depends
496 on pulsation period not on conscious pulse perception. *Physiology and Behavior*, 100(4):327–331.
- 497 [9] Burseg, K. M. M., Brattinga, C., de Kok, P. M. T., and Bult, J. H. F. (2010b). Sweet taste enhancement through pulsatile stimulation depends
498 on pulsation period not on conscious pulse perception. *Physiology and Behavior*, 100(4):327–331.
- 499 [10] Burseg, K. M. M., Camacho, S., and Franciscus, J. H. (2011). Effects of pulsation rate and viscosity on pulsation-induced taste enhancement:
500 New insights into texture - Taste interactions. *Journal of Agricultural and Food Chemistry*, 59(10):5548–5553.
- 501 [11] Burseg, K. M. M., Camacho, S., Knoop, J., and Bult, J. H. F. (2010c). Sweet taste intensity is enhanced by temporal fluctuation of aroma and
502 taste, and depends on phase shift. *Physiology and Behavior*, 101(5):726–730.

- 503 [12] Busch, J. L., Tournier, C., Knoop, J. E., Kooyman, G., and Smit, G. (2009). Temporal contrast of salt delivery in mouth increases salt
504 perception. *Chemical Senses*, 34(4):341–348.
- 505 [13] BVL (2019). Erklärung von Mailand 2019 – 2024. (27.08.2019).
- 506 [14] Cook, D. J., Hollowood, T. A., Linforth, R. S., and Taylor, A. J. (2003). Oral shear stress predicts flavour perception in viscous solutions.
507 *Chemical Senses*, 28(1):11–23.
- 508 [15] Cooper, K. A., Campos-Giménez, E., Alvarez, D. J., Rytz, A., Nagy, K., and Williamson, G. (2008). Predictive relationship between
509 polyphenol and nonfat cocoa solids content of chocolate. *Journal of Agricultural and Food Chemistry*, 56(1):260–265.
- 510 [16] de Boer, G. B., de Weerd, C., Thoenes, D., and Goossens, H. W. (1987). Laser Diffraction Spectrometry: Fraunhofer Diffraction Versus Mie
511 Scattering. *Particle & Particle Systems Characterization*, 4(1-4):14–19.
- 512 [17] De Celis Alonso, B., Marciani, L., Head, K., Clark, P., Spiller, R. C., Rayment, P., Ablett, S., Francis, S., and Gowland, P. A. (2007).
513 Functional magnetic resonance imaging assessment of the cortical representation of oral viscosity. *Journal of Texture Studies*, 38(6):725–737.
- 514 [18] Dijksterhuis, G. and Eilers, P. (1997). Modelling time-intensity curves using prototype curves. *Food Quality and Preference*, 8(2):131–140.
- 515 [19] Du Bois, G. E. and Prakash, I. (2012). Non-caloric sweeteners, sweetness modulators, and sweetener enhancers. *Annual Review of Food
516 Science and Technology*, 3(1):353–380.
- 517 [20] Ehlers, D. (2012). *Controlled Crystallization of Complex Confectionery Fats*. Number 21142.
- 518 [21] Farzanmehr, H. and Abbasi, S. (2009). Effects of inulin and bulking agents on some physicochemical, textural and sensory properties of milk
519 chocolate. *Journal of Texture Studies*, 40(5):536–553.
- 520 [22] Frank, R. A. and Byram, J. (1988). Taste-smell interactions are tastant and odorant dependent. *Chemical Senses*, 13(3):445–455.
- 521 [23] Glumac, M., Qin, L., Chen, J., and Ritzoulis, C. (2019). Saliva could act as an emulsifier during oral processing of oil/fat. *Journal of Texture
522 Studies*, 50(1):83–89.
- 523 [24] Grabenhorst, F., Rolls, E. T., and Bilderbeck, A. (2008). How cognition modulates affective responses to taste and flavor: Top-down influences
524 on the orbitofrontal and pregenual cingulate cortices. *Cerebral Cortex*, 18(7):1549–1559.
- 525 [25] Guinard, J. X. and Mazzucchelli, R. (1999). Effects of sugar and fat on the sensory properties of milk chocolate: Descriptive analysis and
526 instrumental measurements. *Journal of the Science of Food and Agriculture*, 79(11):1331–1339.
- 527 [26] Hallock, R. M. and Di Lorenzo, P. M. (2006). Temporal coding in the gustatory system. *Neuroscience and Biobehavioral Reviews*,
528 30(8):1145–1160.
- 529 [27] Halpern, B. P., Kelling, S. T., and Meiselman, H. L. (1986). An analysis of the role of stimulus removal in taste adaptation by means of
530 simulated drinking. *Physiology and Behavior*, 36(5):925–928.
- 531 [28] Halpern, B. P. and Marowitz, L. A. (1973). Taste responses to lick , duration stimuli. 57(1973):473–478.
- 532 [29] Holm, K., Wendin, K., and Hermansson, A. M. (2009). Sweetness and texture perceptions in structured gelatin gels with embedded sugar
533 rich domains. *Food Hydrocolloids*, 23(8):2388–2393.
- 534 [30] Hutchings, S. C., Low, J. Y., and Keast, R. S. (2019). Sugar reduction without compromising sensory perception. An impossible dream?
535 *Critical Reviews in Food Science and Nutrition*, 59(14):2287–2307.
- 536 [31] Kaneko, R. and Kitabatake, N. (2001). Structure-sweetness relationship in thaumatin: Importance of lysine residues. *Chemical Senses*,
537 26(2):167–177.
- 538 [32] Karalus, M., Pontet, C., and Vickers, Z. (2016). Introduction : - Materials & methods : -. Technical Report 1.
- 539 [33] Khemacheevakul, K., Wolodko, J., Nguyen, H., and Wismer, W. (2021). Temporal sensory perceptions of sugar-reduced 3D printed choc-
540 olates. *Foods*, 10(9):1–14.
- 541 [34] Kistler, T., Pridal, A., Bourcet, C., and Denkel, C. (2021). Modulation of sweetness perception in confectionary applications. *Food Quality
542 and Preference*, 88.
- 543 [35] Koeferli, C. R., Piccinelli, P., and Sigrist, S. (1996). The influence of fat, sugar and non-fat milk solids on selected taste, flavor and texture
544 parameters of a vanilla ice-cream. *Food Quality and Preference*, 7(2):69–79.
- 545 [36] Kokini, J. L. (1987). The physical basis of liquid food texture and texture-taste interactions. *Journal of Food Engineering*, 6(1):51–81.
- 546 [37] Koriyama, T., Wongso, S., Watanabe, K., and Abe, H. (2002). Fatty acid compositions of oil species affect the 5 basic taste perceptions.
547 *Journal of Food Science*, 67(2):868–873.
- 548 [38] LAGUNA, L., FISZMAN, S., and TARREGA, A. (2021). Saliva Matters: Reviewing the role of saliva in the rheology and tribology of liquid
549 and semisolid foods. Relation to in-mouth perception. *Food Hydrocolloids*, 116(December 2020):106660.
- 550 [39] Lawless, H. T. and Heymann, H. (2010). Sensory evaluation of food: principles of good practice.
- 551 [40] Liu, Y. H. and Macfie, H. J. (1990). Methods for averaging time - intensity curves. *Chemical Senses*, 15(4):471–484.
- 552 [41] Marangoni, A. G., Acevedo, N., Maleky, F., Co, E., Peyronel, F., Mazzanti, G., Quinn, B., and Pink, D. (2012). Structure and functionality of
553 edible fats. *Soft Matter*, 8(5):1275–1300.
- 554 [42] Mellers, B. and Birnbaum, M. (1982). Loci of contextual effects in judgement. *Journal of Experimental Psychology*, 4:582–601.
- 555 [43] Mellers, B. and Birnbaum, M. (1983). Contextual effects in social judgement. *Journal of Experimental Psychology*, 19:157–171.
- 556 [44] Miller, K. B., Stuart, D. A., Smith, N. L., Lee, C. Y., McHale, N. L., Flanagan, J. A., Boxin, O. U., and Hurst, W. J. (2006). Antioxidant
557 activity and polyphenol and procyanidin contents of selected commercially available cocoa-containing and chocolate products in the United
558 States. *Journal of Agricultural and Food Chemistry*, 54(11):4062–4068.
- 559 [45] Mishra, K., Grob, L., Kohler, L., Zimmermann, S., Gstöhl, S., Fischer, P., and Windhab, E. J. (2021). Entrance flow of unfoamed and foamed
560 Herschel-Bulkley fluids. *Journal of Rheology*, 65(6):1155–1168.
- 561 [46] Mishra, K., Kummer, N., Bergfreund, J., Kämpf, F., Bertsch, P., Pauer, R., Nyström, G., Fischer, P., and Windhab, E. J. (2023). Controlling
562 lipid crystallization across multiple length scales by directed shear flow. *Journal of Colloid and Interface Science*, 630:731–741.
- 563 [47] Mosca, A. C. and Chen, J. (2017). Food-saliva interactions: Mechanisms and implications. *Trends in Food Science and Technology*,
564 66:125–134.
- 565 [48] Mosca, A. C., Rocha, J. A., Sala, G., van de Velde, F., and Stieger, M. (2012). Inhomogeneous distribution of fat enhances the perception of
566 fat-related sensory attributes in gelled foods. *Food Hydrocolloids*, 27(2):448–455.
- 567 [49] Mosca, A. C., van de Velde, F., Bult, J. H., van Boekel, M. A., and Stieger, M. (2015). Taste enhancement in food gels: Effect of fracture

- 568 properties on oral breakdown, bolus formation and sweetness intensity. *Food Hydrocolloids*, 43:794–802.
- 569 [50] Mosca, A. C., Velde, F. v. d., Bult, J. H., van Boekel, M. A., and Stieger, M. (2010). Enhancement of sweetness intensity in gels by
570 inhomogeneous distribution of sucrose. *Food Quality and Preference*, 21(7):837–842.
- 571 [51] Nitschke, J. B., Dixon, G. E., Sarinopoulos, I., Short, S. J., Cohen, J. D., Smith, E. E., Kosslyn, S. M., Rose, R. M., and Davidson, R. J.
572 (2006). Altering expectancy dampens neural response to aversive taste in primary taste cortex. *Nature Neuroscience*, 9:435–442.
- 573 [52] Noort, M. W. J., Bult, J. H. F., and Stieger, M. (2012). Saltiness enhancement by taste contrast in bread prepared with encapsulated salt.
574 *Journal of Cereal Science*, 55(2):218–225.
- 575 [53] Pareyt, B., Talhaoui, F., Kerckhofs, G., Brijs, K., Goesaert, H., Wevers, M., and Delcour, J. A. (2009). The role of sugar and fat in sugar-snap
576 cookies: Structural and textural properties. *Journal of Food Engineering*, 90(3):400–408.
- 577 [54] Piernas, C., Ng, S. W., and Popkin, B. (2013). Trends in purchases and intake of foods and beverages containing caloric and low-calorie
578 sweeteners over the last decade in the United States. *Pediatric Obesity*, 8(4):294–306.
- 579 [55] Plassmann, H., O'Doherty, J., Shiv, B., and Rangel, A. (2008). Marketing actions can modulate neural representations of experienced
580 pleasantness. *Proceedings of the National Academy of Sciences of the United States of America*, 105(3):1050–1054.
- 581 [56] Prawira, M. and Barringer, S. A. (2009). Effects of conching time and ingredients on preference of milk chocolate. *Journal of Food Processing
582 and Preservation*, 33(5):571–589.
- 583 [57] Ross, M. M., Kelly, A. L., and Crowley, S. V. (2019). *Potential Applications of Dairy Products, Ingredients and Formulations in 3D Printing*.
584 Elsevier Inc.
- 585 [58] Rostagno, W. (1969). Chocolate particles size and its organoleptic influence. *The Manufacturing Confectioner*, pages 81–85.
- 586 [59] Rothkopf, I. and Danzl, W. (2015). Changes in chocolate crystallization are influenced by type and amount of introduced filling lipids.
587 *European Journal of Lipid Science and Technology*, 117(11):1714–1721.
- 588 [60] Sarinopoulos, I., Dixon, G. E., Short, S. J., Davidson, R. J., and Nitschke, J. B. (2006). Brain mechanisms of expectation associated with
589 insula and amygdala response to aversive taste: Implications for placebo. *Brain, Behavior, and Immunity*, 20(2):120–132.
- 590 [61] Savage, G. P., McNeil, D. L., and Dutta, P. C. (1997). Lipid composition and oxidative stability of oils in hazelnuts (*Corylus avellana L.*)
591 grown in New Zealand. *JAOCs, Journal of the American Oil Chemists' Society*, 74(6):755–759.
- 592 [62] Schiffman, S. S., Graham, B. G., Sattely-Miller, E. A., and Peterson-Dancy, M. (2000). Elevated and sustained desire for sweet taste in
593 African-Americans: A potential factor in the development of obesity. *Nutrition*, 16(10):886–893.
- 594 [63] Soltanahmadi, S., Bryant, M., and Sarkar, A. (2022). Insights into the Multiscale Lubrication Mechanism of Edible Phase Change Materials.
595 *ACS Applied Materials and Interfaces*.
- 596 [64] Theunissen, M. J. and Kroeze, J. H. (1996). Mouth movements diminish taste adaptation, but rate of mouth movement does not affect
597 adaptation. *Chemical Senses*, 21(5):545–551.
- 598 [65] Upadhyay, R. and Chen, J. (2019). Smoothness as a tactile percept: Correlating ‘oral’ tribology with sensory measurements. *Food
599 Hydrocolloids*, 87(July 2018):38–47.
- 600 [66] Van Malssen, K., Peschar, R., and Schenk, H. (1996). Real-time X-ray powder diffraction investigations on cocoa butter. II. The relationship
601 between melting behavior and composition of β -cocoa butter. *JAOCs, Journal of the American Oil Chemists' Society*, 73(10):1217–1223.
- 602 [67] Verhagen, J. V. and Engelen, L. (2006). The neurocognitive bases of human multimodal food perception: Sensory integration. *Neuroscience
603 and Biobehavioral Reviews*, 30(5):613–650.
- 604 [68] Wilton, M., Stancak, A., Giesbrecht, T., Thomas, A., and Kirkham, T. (2019). Intensity expectation modifies gustatory evoked potentials to
605 sweet taste: Evidence of bidirectional assimilation in early perceptual processing. *Psychophysiology*, 56(3):1–12.
- 606 [69] Woods, A. T., LLoyd, D. M., Kuenzel, J., Poliakoff, E., Dijksterhuis, G. B., and Thomas, A. (2011). Expected taste intensity affects response
607 to sweet drinks in primary taste cortex. *NeuroReport*, 22:365–369.
- 608 [70] Wu, S., Burns, S. A., Reeves, A., and Elsner, A. E. (1996). Flicker brightness enhancement and visual nonlinearity. *Vision Research*,
609 36(11):1573–1583.
- 610 [71] Zorn, S., Alcaire, F., Vidal, L., Giménez, A., and Ares, G. (2014). Application of multiple-sip temporal dominance of sensations to the
611 evaluation of sweeteners. *Food Quality and Preference*, 36:135–143.